MICROWAVE IMAGING OF DEFECTS IN GRAPHITE REINFORCED COMPOSITE MATERIALS

R.P. Flam and B.W. Deats

Flam & Russell, Inc.
P.O. Box 999
Horsham, PA 19044

INTRODUCTION

In an effort to develop and evaluate new non-destructive evaluation (NDE) techniques for resin-matrix composites, we have investigated the feasibility of utilizing electromagnetic imaging for materials evaluation and has demonstrated the ability of existing electromagnetic imaging techniques to detect and locate flaws within carbon-epoxy samples. This paper presents the technical issues associated with using electromagnetic imaging for NDE measurements. These include the selection of test frequencies, sample orientation, signal processing techniques, and the impact of material properties on the measurement results. Measured results are presented for carbon-epoxy material samples.

IMAGING TECHNIQUE

The basic Inverse-Synthetic Aperture Radar (ISAR) imaging technique is described in many standard texts, and a good introduction is given in reference one. In ISAR imaging, data on the amplitude and phase of target reflection is obtained at a variety of frequencies and aspect angles. This data is then transformed into a reflectivity map in range and cross-range coordinates. The underlying assumptions behind the transformation are that the target consists of an ensemble of broadband, isotropic non-interacting point scatterers.

In order to achieve downrange resolution, data is taken at a number of equally spaced frequencies across the bandwidth, B. This complex reflection data can be Fourier transformed from the frequency domain to the time domain. The downrange resolution achievable is related to the bandwidth used in the measurement by the equation:

$$R = \frac{C}{(2B)} \qquad (1)$$

where C is the velocity of propagation in the medium. Clearly physical resolution is improved for propagation in dielectric media, relative to free space, by the reduced value of C.

The Fourier transform from frequency to time domain makes use of the variation of reflected phase with frequency to distinguish between scatterers at different ranges. In an analogous way, cross range resolution can be obtained by rotating the target around an axis of rotation near the center of the target. For a scatterer at the axis of rotation, the phase of the scattered signal is independent of aspect angle. For a scatterer located at a

Review of Progress in Quantitative Nondestructive Evaluation, Vol. 11
Edited by D.O. Thompson and D.E. Chimenti, Plenum Press, New York, 1992

distance, D, from the axis of rotation the reflected phase will vary with aspect angle and the magnitude of the variation will be proportional to D. This variation of reflected phase can again be transformed to give cross range resolution. The resolution in the cross range dimension is given by the equation:

$$X = \frac{\lambda}{4\ SIN\left(\frac{\theta}{2}\right)} \qquad (2)$$

Where λ is the wavelength of the signal being measured and θ is the angular region (in radians) over which measure- ments are made. As described in reference 1, if a simple 2-dimensional Fourier transform is used to convert data measured in the frequency-angle domain to the range-cross range domain, smearing of the image will occur which is proportional to the distance from the center of rotation. This smearing is usually referred to as "defocusing". By using a more rigorously correct form of the 2-dimensional transformation an image which maintains its sharpness over the entire field of view can be generated. The algorithm utilized in this focusing process is a form of polar to rectangular transformation. This transformation requires a 2-dimensional interpolation of the data prior to the 2-dimensional Fourier transform. The techniques and algorithms used in image formation have been well developed at FR, and have been used extensively in the evaluation of radar cross section of a wide variety of targets.

DESIGN TRADEOFFS

Figure 1 shows the predicted depth of penetration to a level of -25 dB for three selected materials. This energy level represents, based on laboratory measurements at FR, the maximum one-way attenuation which can be tolerated in a scattering measurement and still yield predictable, accurate results. From these curves, it is apparent that the greatest energy penetration, and hence sensitivity, occurs with lower frequencies of incident electromagnetic energy. At higher frequencies, penetration depths of 10 to 20 inches are still possible for low conductivity dielectrics. Performing the same calculations for pure, homogeneous carbon yields a worst-case estimate of the penetration depth for carbon-epoxy laminates. The greatly reduced penetration depth for pure carbon (approximately 10^{-8} inches) is due to the extremely high conductivity of this material. For this reason, electromagnetic imaging is not a good candidate for NDE testing on pure carbon samples.

Carbon-epoxy laminates, however, do not consist entirely of pure homogeneous carbon. In fact, these materials are quite inhomogeneous as the layers of conductive carbon are separated by a dielectric resin. One would expect the performance of this composite material to fall somewhere between the two sets of curves for dielectrics and conductors. Results from laboratory measurements which correlate with this prediction are presented below.

Summarizing this section, it is apparent that an image center frequency selected as low as possible will provide the greatest NDE sensitivity to defects located within the test sample.

In general, greater measurement bandwidths are possible at higher measurement frequencies. For example, a 120 percent image measurement bandwidth centered at 1 GHz yields a 1.2 GHz bandwidth while a measurement centered at 10 GHz yields a 12 GHz bandwidth. From Equation (1), the improvement in image resolution is directly proportional to this bandwidth. To achieve the best image resolutions, the NDE measurement should be performed with the highest feasible center frequency. However, it is also desirable to perform the measurement with the lowest possible center frequency to achieve the maximum penetration depths. Figure 2 shows the effect of the electric constant on the down-range resolution. The resolution values shown indicate the size of range 'bins' in a one-dimensional Fourier transform based on 120 percent of bandwidth at the specified center frequency. Two-dimensional, square pixel, image-domain pixel sizes

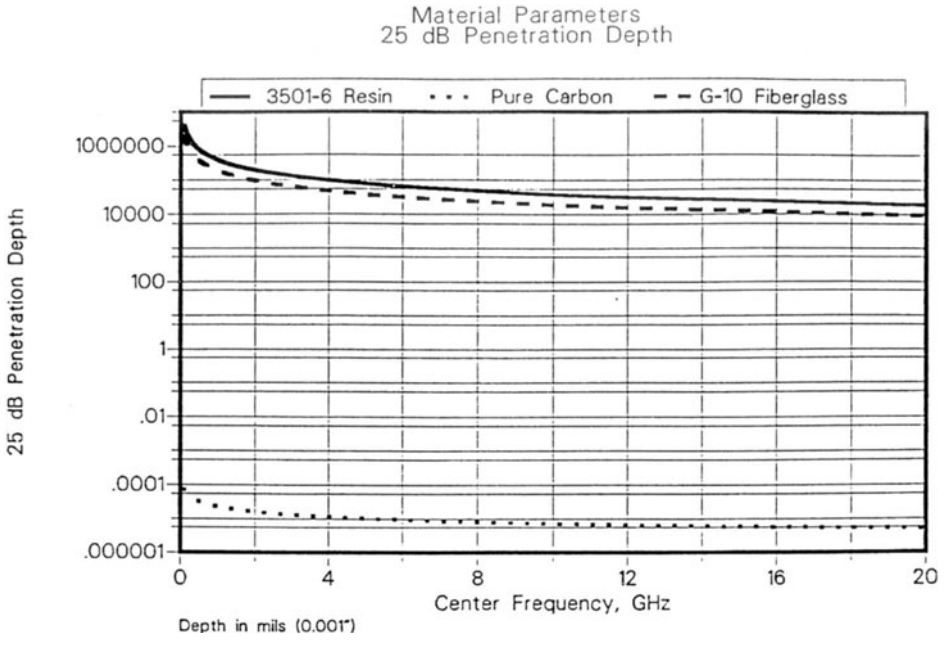

Figure 1. Relative penetration depths of three selected materials

can be calculated by multiplying the indicated one-dimensional resolutions by a factor of 1.56. This increase in pixel size is due to data re-sampling to obtain the rectangular image from rotational data.

Combining Figures 1 and 2, a relationship between measurement resolution and penetration depth within the sample results as shown in Figure 3. The left-hand side of these curves is obtained for RF frequencies of 20 GHz. The right-hand side of these curves results from illumination frequencies of approximately 2 GHz. Using this curve, a center frequency may be selected which yields the desired penetration and resolution for the particular material under test.

MEASUREMENT RESULTS

To empirically verify the relationships outlined in the previous section, actual NDE laboratory measurements were performed on both dielectric and graphite-epoxy test samples. These tests provide insight not only into the characteristics of the individual samples, but also aid in the development of optimal test techniques.

The composite samples under evaluation were provided by the Naval Air Development Center (NADC) in Warminster, PA. These samples measure approximately four by eight inches (rectangular) and are approximately 0.125 inches thick. The first sample, referred to as sample 'A', is slightly curved along its longest dimensions with an approximate radius of curvature of 100 inches. This yields a maximum out-of-plane displacement of 0.075 inches at the center of the sample. Each ply within this sample is made up of 'AS-4' carbon fiber with a diameter of approximately 12 microns. There are 12,000 to 20,000 fibers per 'tow', with each fiber coated with a dielectric polymer. The fibers are bonded together to form a ply having a total thickness of 0.005 to 0.006 inches. The resin used to bond the fibers into plys is a type 3501-6 epoxy. Sample 'A' consists of plys whose carbon fiber orientation is along the panel's shortest dimension.

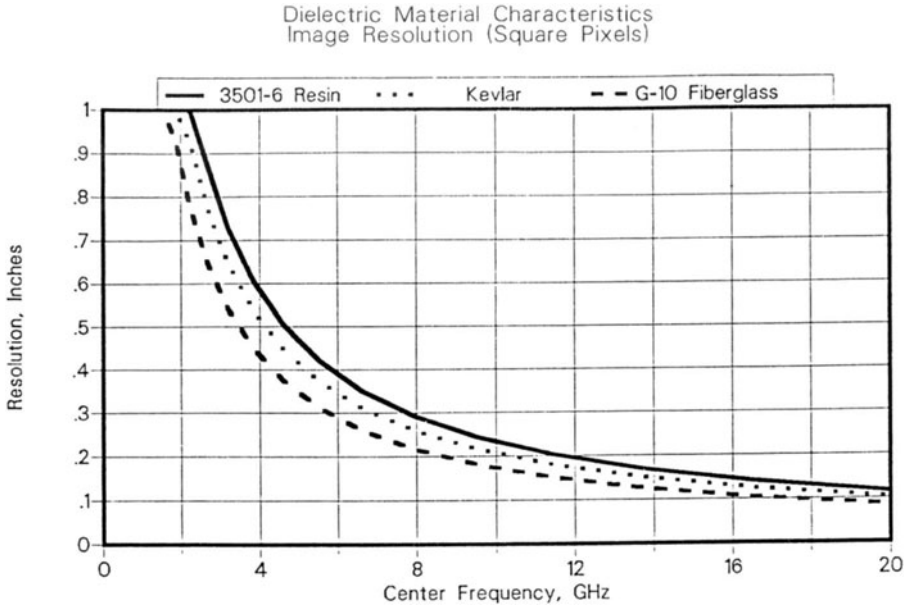

Figure 2. Range resolutions for selected dielectric materials

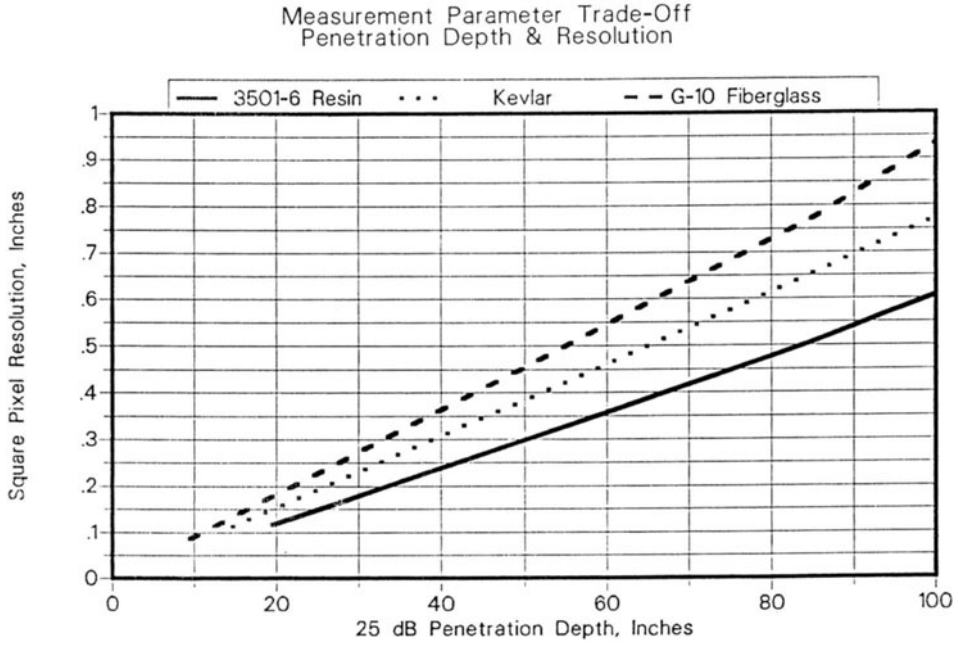

Figure 3. NDE measurement design curve showing the relationship of image resolution and material penetration depth for selected dielectric materials

The second sample (sample 'B') has the same physical dimensions as sample 'A' with the exception of panel flatness. Panel 'B' is planar rather than curved. Additionally, the fiber orientation in panel 'B' is at a 45 degree orientation relative to the panel edges. Each laminate ply has the fiber orientation placed orthogonal to the adjacent plys. With the above exceptions, sample 'A' and sample 'B' differ only in the location and type of possible defects within their structure.

The measurement instrumentation system utilized for these tests is very similar to that used in the FR Model 8003 RCS Measurement System. The measurement receiver is the model 8510 network analyzer which provides excellent stability and I/Q dynamic range and accuracy. A Model 8105B Pulse Modulator is used to enhance the HP8510's measurement capability as a radar transmitter and receiver. This module provides RF power amplification, receive low-noise amplification, as well as pulse modulation and receive gating. The resulting measurement system provides the following system performance levels:

Frequency Coverage	2-18 GHz
Transmit Power (Peak)	+20 dBm
Dynamic Range (128 Avg.)	110 dB
Receiver Sensitivity (CW)	-120 dBm
Minimum Gate Physical Gate Width	5 nS, Typ
Minimum Processed Gate Width	0.2 nS

A DEC Micro VAX II computer provides the necessary control of data acquisition operating both the synthesized frequency source, 8510 receiver, and FR model 8502 positioner controller. The FR8003/RCS measurement software coordinates the target movement and data acquisition while collecting the requested scattering data. Typically, swept frequency data is gathered over a range of angles thus providing the necessary data to perform both one and two-dimensional scattering image analysis. The necessary error correction, calibration and image formation is performed by the FR Pro and CRIP software packages developed by FR.

The above measurement system is connected to a 10' x 10' x 22' shielded anechoic chamber capable of measuring targets up to three feet in cross-section. The walls of this chamber are covered with radar absorbing material (RAM) to minimize undesired reflections within the range. Illuminating the range are two FR Model 6414 Diagonal Horn Antennas operated in a quasi-monostatic configuration. These antennas provide a near constant and symmetric E- and H-plane beamwidth over the frequency range of 6 to 18 GHz.

Figure 4 shows the results of the sample 'B' panel measurement when processed through the FR CRIP software. This chart may be interpreted as though the radar is located at the bottom of the figure and the scattering information is presented from a 'top view'. Distances on this chart are one-way path lengths. Multiple bounces around the panel are apparent as panel-wide responses falling just behind the primary panel response. It is apparent from this data set that the specularly reflected energy from the graphite-epoxy panels is blinding the radar from seeing any potential defects within the material. For this reason, off-normal imaging measurement were made. Using this technique, the large specular response from the panel is reflected into the RAM on the sidewalls of the anechoic chamber where it is absorbed. Energy still returns to the radar from the leading and trailing edges of the panel. However, between these two edges, a 'quiet' region should exist where energy propagates along the panel surface without reflection. If a defect exists within the sample, image representation for the panel will indicate a reflection.

Figure 5 shows the resulting image for an aluminum reference panel cut to match the dimensions of the test panels. The reference panel is imaged about an aspect angle of 40 degrees from specular. As expected, no defects are indicated on this panel. A third response is indicated in the image which lies directly behind the sample plate. This response results from the energy which reflects from the leading edge of the panel down to the trailing edge, and then diffracts back to the radar. Because this response is due to a multiple reflection between the leading and trailing edges, the path length of this ray path

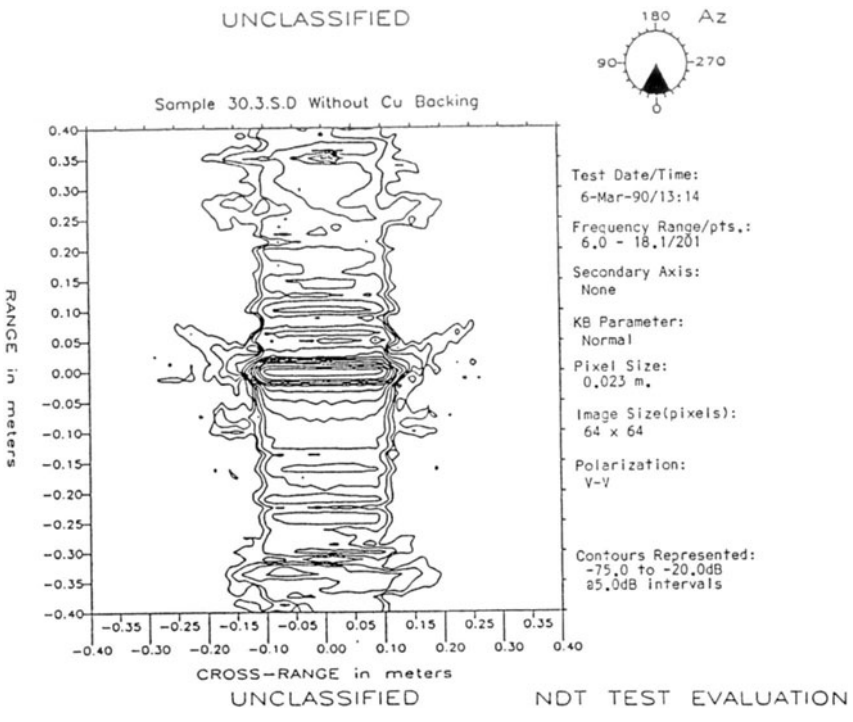

Figure 4. Electromagnetic image of sample 'B' measured from 6 to 18 GHz

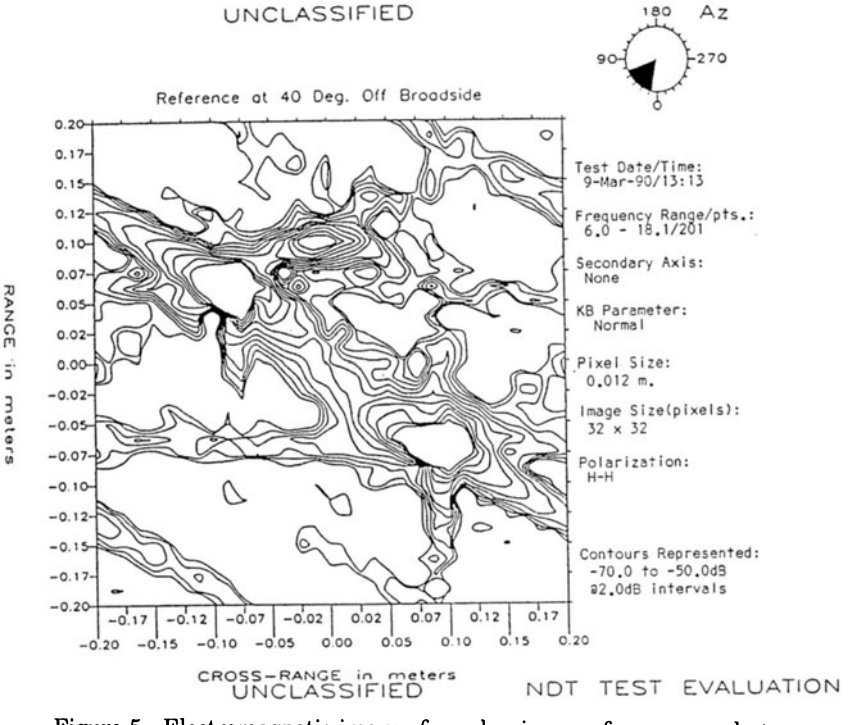

Figure 5. Electromagnetic image of an aluminum reference panel at a 40 degree aspect angle measured from 6 to 8 GHz

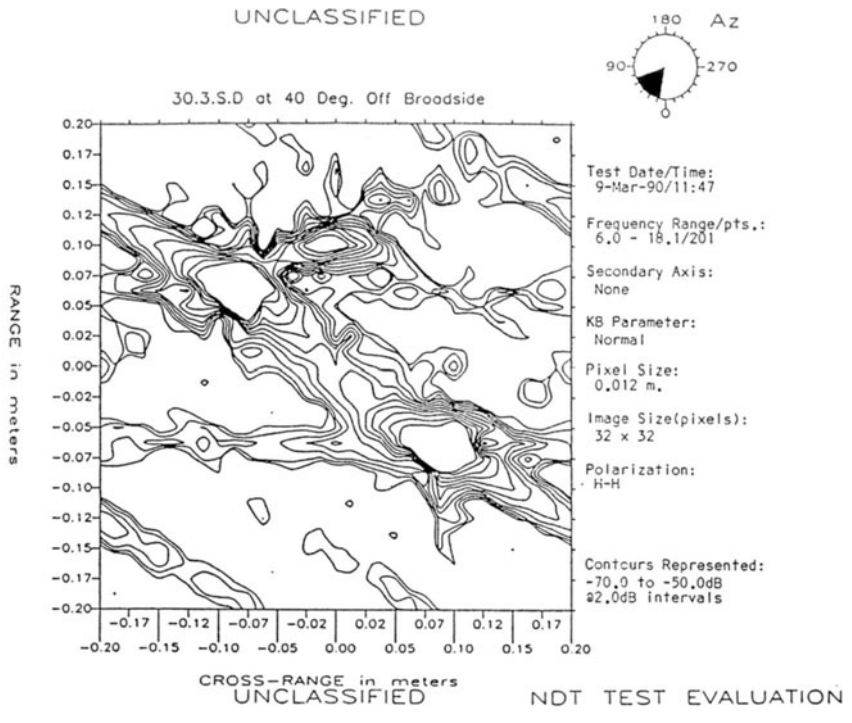

Figure 6. Electromagnetic image of sample 'B' at a 40 degree aspect angle measured from 6 to 8 GHz

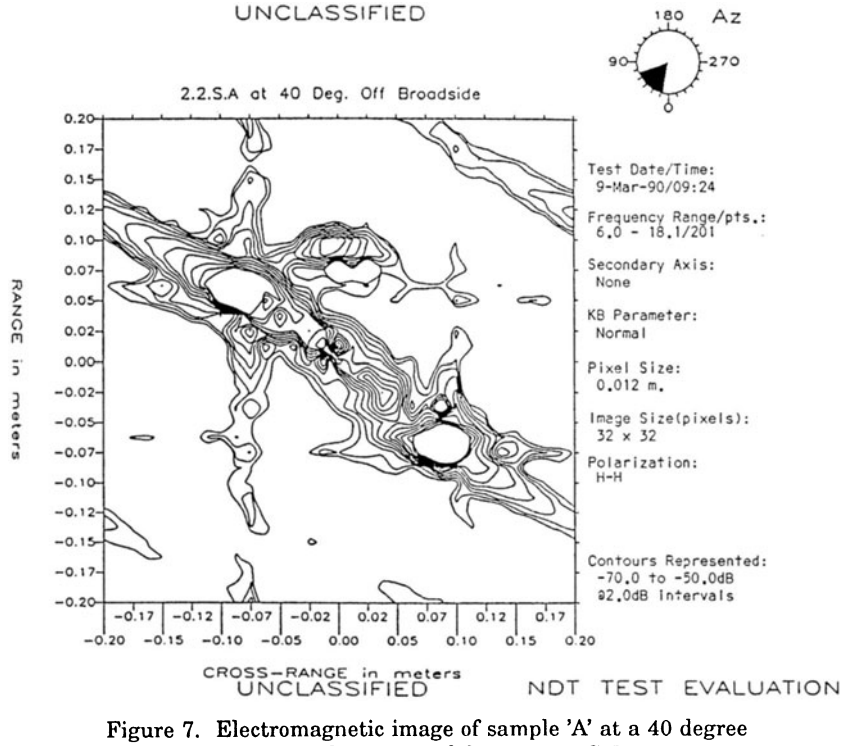

Figure 7. Electromagnetic image of sample 'A' at a 40 degree aspect angle measured from 6 to 8 GHz

does not change with rotation. For this reason, the response appears directly behind the sample. The down-range location of this response is determined by the path length the ray travels along the sample between the two edges. The slight offset of this multiple reflection response on the image is due to a slight error in the target mounting which placed the target center slightly off of the axis of rotation.

Figure 6 shows the same measurement on sample 'B'. A slight difference in the scattering return from the central region of the sample is apparent. However, no clear defects or anomalies can be identified in comparing this sample's measured response to the reference plate measured response.

Figure 7 shows the image result obtained for sample 'A'. Unlike the previous two samples, this panel shows a significant return from two regions along the surface of the panel. Two measured responses approximately 2.5 times stronger than the background clutter are apparent with a separation of 2.75 inches. No visible defects are indicated on this measured sample at these locations. The origin of the indicated scattering responses is believed to be due to energy reflecting from two discontinuities just beneath the surface of the material which are not visibly apparent. A defect producing this type of scattering under this incidence angle would be a broken laminate ply, discontinuities in some or all of the carbon fibers within a ply, or a delamination between two plys at or near the sample surface.

The ability to detect differences in responses between geometrically similar samples suggests that electromagnetic energy is penetrating the surface of the carbon epoxy laminate. Under normal incidence, the reflection from the surface of the material obscures the relatively small signal which penetrates, and then reflects, from the material surface. At off-normal incidence, however, the specular reflection is not directly incident upon the measurement system and a much greater measurement sensitivity is realized.

The region within the sample surface over which effective NDE testing may be performed may be significantly increased by reducing the direct scattering from the edges of the sample under test. As the images show, a portion of the sample panel is obscured at either end of the panel by the finite impulse response width of the leading and trailing edge reflections. Placing these samples within a shaped test fixture will reduce, or possibly eliminate, these reflections thus allowing for defect detection over the entire extent of the test sample.

CONCLUSION

Microwave imaging as an NDE measurement tool has been shown to be a viable addition to the currently available NDE measurement processes, especially for materials with low to moderate bulk conductivities. Measured results on carbon-epoxy laminate samples indicate an ability to detect defects even in highly conductive materials. This ability is due largely to the bulk electrical characteristics of the carbon epoxy combination to be significantly less conductive than pure carbon.

ACKNOWLEDGEMENT

This work has been performed under contract issued by the Naval Air Systems Command (NASC).

REFERENCE

1. "High Resolution Radar Imaging", D.L. Mensa, Artech House, Dedham, MA; Chapter 4.